

1 **Glacier extent and climate in the Maritime Alps during the Younger Dryas**

2 Matteo Spagnolo¹, Adriano Ribolini²

3 ¹ School of Geosciences, University of Aberdeen (UK) (corresponding author: m.spagnolo@abdn.ac.uk)

4 ² Dipartimento di Scienze della Terra, Università di Pisa (Italy)

5

6 Keywords: Younger Dryas; glacier reconstruction; equilibrium line altitude; palaeoclimate;
7 cosmogenic dates; Maritime Alps

8

9 Abstract

10 This study focuses on an Egesen-stadial moraine located at 1906-1920 m asl in the NE Maritime Alps,
11 Europe. Three moraine boulders are dated, via cosmogenic isotope analyses, to $12,490 \pm 1120$, $12,260$
12 ± 1220 and $13,840 \pm 1240$ yr, an age compatible with the Younger Dryas cooling event. The
13 reconstructed glacier that deposited the moraine has an equilibrium line altitude of 2349 ± 5 m asl,
14 calculated with an Accumulation Area Balance Ratio of 1.6. The result is very similar to the equilibrium
15 line altitude of another reconstructed glacier that deposited a moraine also dated to Younger Dryas,
16 in the SW Maritime Alps. The similarity suggests comparable climatic conditions across the region
17 during the cooling event. The Younger Dryas palaeoprecipitation is 1549 ± 26 mm/yr, calculated using
18 the empirical law that links precipitation and temperature at a glacier equilibrium line altitude, with
19 palaeotemperatures obtained from nearby palynological and chironomids studies. The
20 palaeoprecipitation is similar to the present, thus indicating non-arid conditions during the Younger
21 Dryas. This is probably due to the Maritime Alps peculiar position, at the crossroads between air
22 masses from the Mediterranean and the North Atlantic, the latter displaced by the southward
23 migration of the polar front. The equilibrium line altitude interval defined by the two reconstructed
24 glaciers, is used to model the extent of another 66 potential Younger Dryas glaciers in the region. Each
25 modelled glacier is reconstructed by iteratively changing the position of its front until the
26 reconstructed glacier has an ELA that falls within the interval. The result, which is checked against
27 geomorphological evidence, shows that glaciers covered 83.74 km^2 during the Younger Dryas, with a
28 volume of 5.39 km^3 . All valley heads were occupied by ice, except for the Maddalena/Larche Pass
29 (1999 m asl), an ideal site for future archaeological, palaeoecological and palaeozoological studies.

30

31

32 1. Introduction

33 The Younger Dryas (YD) is the most recent time in our planet's history during which a cooling
34 of the order of some degrees affected a large portion of the Earth, triggered by several climatic
35 processes (Renssen et al., 2015). It occurred at the end of the last glacial period, between 12.9 and
36 11.7 kyr (e.g. Johnsen et al., 2001; Broecker et al, 2010). The critical assemblage of several sources has
37 suggested that the cooling magnitude of this event was of the order of $2-8^\circ \text{ C}$ in the Northern
38 Hemisphere (Shakun and Carlson, 2010), with variations likely controlled by local climatic factors. One

39 of the most evident effects of the YD cooling on the Earth's surface is the widespread advancement
40 of alpine glaciers and the deposition of moraines. The lack of post-YD cooling events of similar or larger
41 magnitude, means that YD moraines are usually well preserved, as they have not been destroyed or
42 remoulded by the overriding of later glacier advances. Indeed, moraines dated back to the YD can be
43 found in many alpine regions worldwide (Ehlers and Gibbard, 2004). The European Alps are one of the
44 first regions where YD moraines have been identified and dated. Here, moraines belonging to the
45 Alpine glacier advance (or chronology stadial) known as the Egesen stadial have been recognised and
46 studied for a long time (e.g. [Heuberger, 1968](#); [Patzelt, 1972](#)). The age of the Egesen moraines has been
47 attributed to the YD, initially via morphotratigraphic reconstructions and, in recent decades, by means
48 of cosmogenic isotope nuclide dating techniques (e.g. [Ivy-Ochs et al., 1996](#); [2009](#)).

49 Frontal (terminal) moraines are the essential ingredient for the reconstruction of former
50 Alpine glaciers, as they indicate the furthest downvalley position (limit or margin) of the glacier.
51 Models can be applied to reconstruct the full extent of palaeo glaciers, given the location of a frontal
52 moraine and the present-day topography, assuming the latter has not undergone intense post-glacial
53 modifications (e.g. [Benn and Hulton, 2010](#)). The ice surface distribution per elevation (hypsometry) of
54 reconstructed glaciers can then be used to extract a palaeo Equilibrium Line Altitude (ELA), the
55 elevation on a glacier where ice ablation and accumulation are equal ([Osmaston, 2005](#)). Modern
56 glacier ELAs have been empirically demonstrated to relate to climate, precipitation and temperature
57 in particular (e.g. [Ohmura et al., 1992](#)). Thus, a palaeo ELA obtained from a glacier reconstruction
58 based on a dated glacial deposit can be used to infer the climatic conditions at the time of deposition
59 of the moraine (e.g. [Hughes et al., 2007](#)).

60 In order to fully analyse the palaeogeography of an alpine region and to quantify palaeo ice
61 extent and volume at a specific time, ideally all palaeoglaciers occupying the region at that time should
62 be reconstructed. Examples of region-wide glaciers reconstruction in alpine contexts exist, but are
63 usually limited to large ice caps and ice fields modelling exercises, more or less constrained by terrain
64 evidence (e.g. for the last glacial cycle in the Alps: [Seguinot et al., 2018](#); for the LGM in the Alps:
65 [Florineth and Schlüchter, 1998](#); [Bini et al., 2009](#); [Ehlers and Gibbard, 2004](#); for the YD in Scotland:
66 [Golledge et al., 2008](#); [Boston et al., 2015](#)). Regional model reconstructions are useful not only to gain
67 insight into the glaciological response to past climate changes but also to understand human activities
68 and behaviours (migrations, trading, land reclamation etc.) (e.g. [Catto et al., 1996](#); [Meyer et al., 2009](#);
69 [Ravazzi et al., 2007](#); [Serrano et al., 2015](#)), as well as fauna and flora dynamics (e.g. extinctions, glacial
70 refugia, etc.) (e.g. [Badino et al., 2018](#); [Casazza et al., 2016](#); [Garnier et al., 2004](#); [Schönswetter et al.,](#)
71 [2005](#); [Schorr et al., 2013](#); [Stehlik, 2003](#)). They also provide essential information to explain changes or

72 hiatuses in other palaeoclimate proxies, for example in alpine lake deposits and speleothems (e.g.
73 [Spotl and Mangini, 2007](#); [van der Bilt et al., 2018](#); [Isola et al., 2019](#)).

74 Here, we present an Egesen moraine in the Maritime Alps (southwestern-most European Alps)
75 dated to the YD by means of cosmogenic isotope analyses. We reconstruct the extent of the glacier
76 that deposited the moraine and we calculate its ELA. The result is combined with the ELA of another,
77 already reconstructed glacier, which deposited the YD-dated Pian del Praiet (PDP) moraine ([Federici
78 et al., 2008](#)), located some 40 km ESE, to define a regional YD ELA for the Maritime Alps. This is used
79 to extract the palaeoclimate conditions of the region at the YD and to reconstruct all potential YD
80 glaciers (66) in one of the main valley systems of this Alpine sector.

81

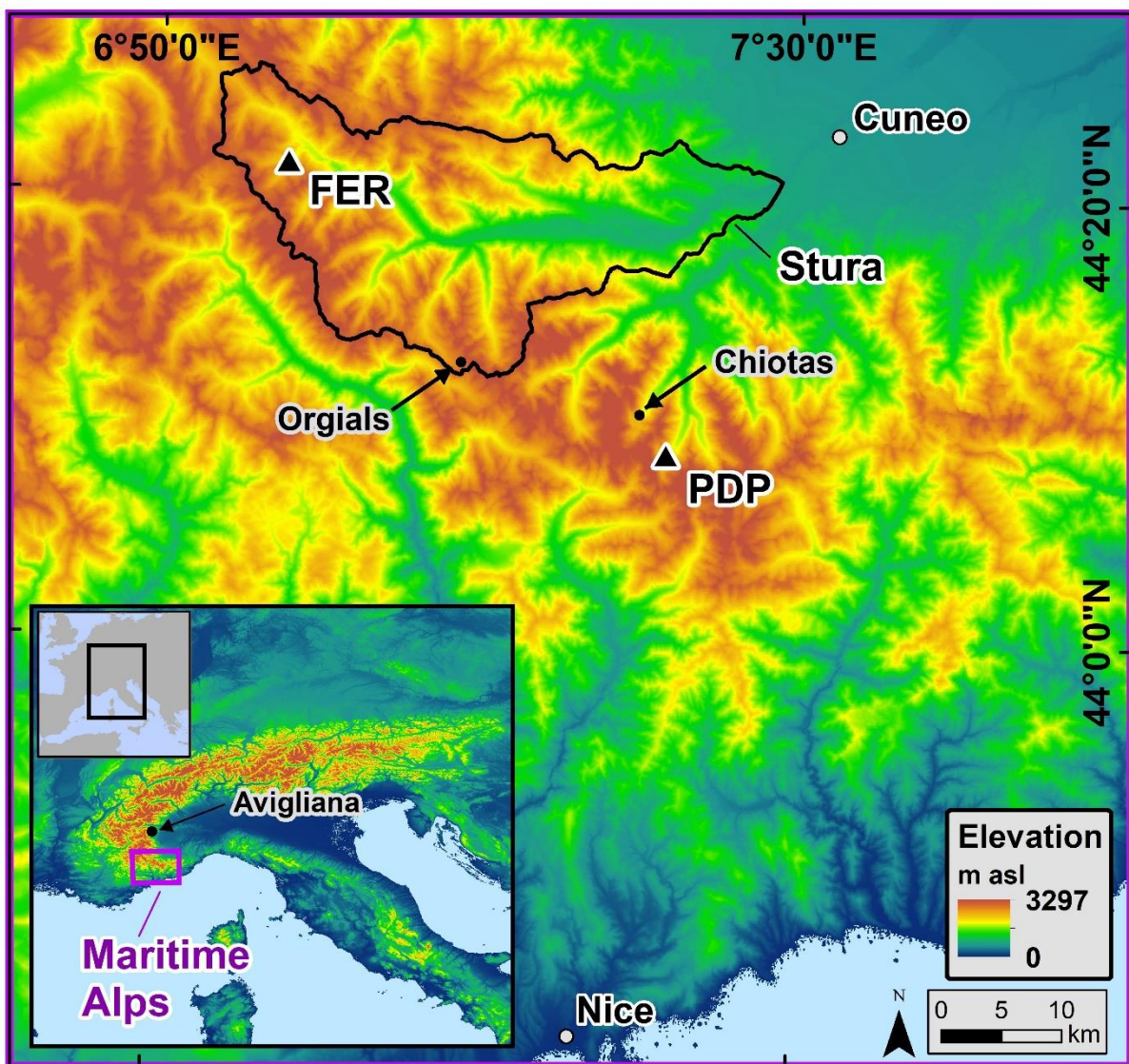
82

83 2. Regional context

84 The Maritime Alps are the southernmost (latitude of 43.9-44.4° N; longitude of 6.9-7.6° E)
85 portion of the European Alps, very close (40-60 km) to the Mediterranean Sea (hence the term
86 “Maritime”) and yet with elevations exceeding 3000 m asl (Figure 1). They are drained by four rivers,
87 which give name to the four main valleys of the region. These are the Tinée, Vesubié, Gesso and Stura
88 (di Demonte) rivers. The first two are located on the southwestern side of the Maritime Alps and drain
89 southward to the Ligurian Sea, while the last two, located on the northeastern side, ultimately drain
90 eastward, into the Po River and the Adriatic Sea. The Maritime Alps have been extensively glaciated
91 during Marine Isotope Stage 2, in line with the global Last Glacial Maximum (26-19 kyr) ([Clark et al.,
92 2009](#); [Shakun and Carlson, 2010](#); [Hughes et al., 2013](#)), when glaciers covered all main valleys and
93 extended towards, but did not reach, the Po Plain (Italy) to the north and the coast near Nice (France)
94 to the south ([Bigot-Cormier et al., 2005](#); [Federici et al., 2012](#)). While a number of moraines mapped in
95 the Maritime Alps have been hypothesised to belong to the Late Pleistocene ([Federici et al., 2003](#)),
96 only PDP moraine, located in the Gesso catchment, has so far been dated to the YD event (average
97 age of 13.2 ± 0.9 kyr) ([Federici et al., 2008](#); [2017](#)).

98 Present-day precipitations are bimodal, with peaks in spring and autumn, and are generally
99 lower than in the nearby northern Apennines and the rest of the Alps ([Isotta et al., 2014](#)).
100 Temperatures are unimodal with a summer peak, and generally higher than in other, nearby Alpine
101 regions ([Durand et al., 2009](#)). Differences exist across the main divide, with the southern side of the
102 Maritime Alps generally characterised by warmer temperatures than in the northern side ([Auer et al.,
103 2007](#)). However, within the studied region of interest, which lies entirely in the northern sector, similar
104 present-day climate conditions exist. This work focuses on the Stura catchment (Figure 1), one of the
105 largest in the southwestern Alps, comprising dozens of Alpine glacial valleys (currently ice-free),

106 covering an area of 615 km². The southern sector of the Stura catchment is generally characterised by
107 the crystalline rocks of the Argentera Massif, while its northern sector is made of sedimentary and
108 metasedimentary rock units (Malaroda et al., 1970). Tectonics has played a key control function on
109 the geometry development of these valleys (Ribolini, 2000; Musumeci et al., 2003, Ribolini and
110 Spagnolo, 2008). The dated moraine presented in this paper is in the Forneris Valley (Figure 1), in the
111 northern sector of the Stura catchment, at an elevation of 1908-1922 m asl. The upper valley, 3-3.5
112 km from the moraine, is characterised by peaks reaching >2700 m asl and comprises four glacial
113 cirques and a number of rock glaciers and glacial deposits. The specific lithology of the Forneris Valley
114 comprises high-grade schist, migmatite and quartzite rocks (Malaroda et al., 1970).
115



116
117 Figure 1. An overview of the Maritime Alps and the Stura catchment within it (outlined in black). The location of
118 the two moraines discussed in the text, PDP and FER (the latter in the Forneris Valley), is indicated, as well as
119 that of the chironomid site of Lago Piccolo di Avigliana ("Avigliana" in the figure), the pollen site of Laghi
120 dell'Orgials ("Orgials"), and the present-day weather station of the Diga del Chiotas ("Chiotas"). The cities of
121 Nice and Cuneo are shown to provide geographical references. The Mediterranean Sea is evidenced in light blue.

122

123 3. Methods

124 3.1 Chronology

125 The Ferrere (FER) moraine is located in the Forneris Valley, Stura catchment, near the village
126 of Ferrere (Figure 1). A total of 10 samples were collected from the moraine during two field
127 campaigns in 2011 and 2013. The <3-cm-thick samples were collected with hammer and chisel from
128 the upper, gently-sloping or horizontal, surface of large gneiss boulders located along the moraine
129 crest and emerging more than 1.5 m above the ground (Table 1 and Figure 2). Samples were crushed
130 and quartz grains extracted by using the standard ^{10}Be cosmogenic isotope analysis procedure (Kohl
131 and Nishizumi, 1992). Only 3 of the 10 samples revealed enough quartz of the right grain size for the
132 content of the isotope ^{10}Be to be measured. Measurements took place at the Natural Environment
133 Research Council - Cosmogenic Isotope Analysis Facility in the UK, with the use of the $2.79 \cdot 10^{-11}$
134 $^{10}\text{Be}/^9\text{Be}$ of Nishiizumi et al. (2007) for NIST 206 SRM4325 (NIST_27900 standardisation code,
135 equivalent to 07KNSTD). Reported exposure ages are calculated with the CRONUS-earth online
136 calculator version 2.3, using a default calibration data set and the time-independent Lal/Stone
137 spallation scheme.

138

139 3.2 Glacial reconstruction and ELA calculation

140 Glacier reconstructions in this paper are based on the application of a dedicated GIS tool,
141 “GlaRe” (Pellitero et al., 2016). The tool creates a 3D glacier surface based on the lateral interpolation
142 of a 2D glacier equilibrium profile, which is calculated by using a plastic rheology glacier model along
143 a user-defined flowline(s) (Benn and Hulton, 2010; Paterson, 1994, p.240; Shilling and Hollin, 1981).
144 Glaciers are reconstructed by extrapolating the ice thickness along the defined flowlines every 5 m,
145 and by applying a default shear stress of 100 kPa. Shape (F) factors (usually between 1 and 5),
146 accounting for the width of the glacial valley, are also included where appropriate, i.e. at different
147 points of valley narrowing. For each reconstructed glacier, the final GlaRe output is a 3D glacier terrain
148 model, which is obtained by interpolating sideways the ice thickness calculated along the flowlines,
149 using a “TOPOtoRASTER” interpolation approach (Pellitero et al., 2016). The reconstructed 3D glacier
150 terrain model is then used to extract the ELA of the glacier, through a separate GIS tool (Pellitero et
151 al., 2015). While the tool allows for most ELA calculation techniques to be implemented, for the sake
152 of consistency all our ELA calculations are based on the same technique, that of the Accumulation
153 Area Balance Ratio (AABR) (Furbish and Andrews, 1984), with an AABR value of 1.6, as recommended
154 for the Alps (Rea; 2009). AABR is considered one of the most robust techniques because it takes into
155 consideration both the hypsometry of the glacier surface (Osmaston, 2005) and the mass balance

156 gradients (Benn and Lehmkuhl, 2000). A contour interval of 10 m is set for the calculation of the glacier
157 surface area, meaning that all extrapolated ELA values have an associated calculation interval of ± 5
158 m (Pellitero et al., 2015).

159 A regional YD ELA interval is defined, based on the two ELAs values relative to glaciers that
160 deposited moraines dated to the YD (PDP and FER) in the Maritime Alps. The YD PDP moraine (Federici
161 et al., 2008) is located ~ 40 km to the SE of the FER moraine (Figure 1). The YD ELA interval is then used
162 to model the extent of all Stura catchment potential YD glaciers, which are largely located between
163 the two dated moraines (Figure 1). The modelled reconstruction is based on the application of the GIS
164 GlaRe and ELA tools (Pellitero et al., 2015, 2016) to all Stura glacial valleys. For each valley the tools
165 are run multiple times, iteratively moving up- or down-valley the hypothetical position of a glacier
166 front, until the reconstructed glacier returns an ELA value that fits within the defined regional YD ELA
167 interval. The approach is similar to that of Rea and Evans (2007) but is improved by the employment
168 of the GIS tools. The modelled position of the glaciers front was checked against evidence of frontal
169 moraines and glacial deposits from field observations, geological maps (Malaroda et al., 1970) and
170 remote sensing (Google Earth™).

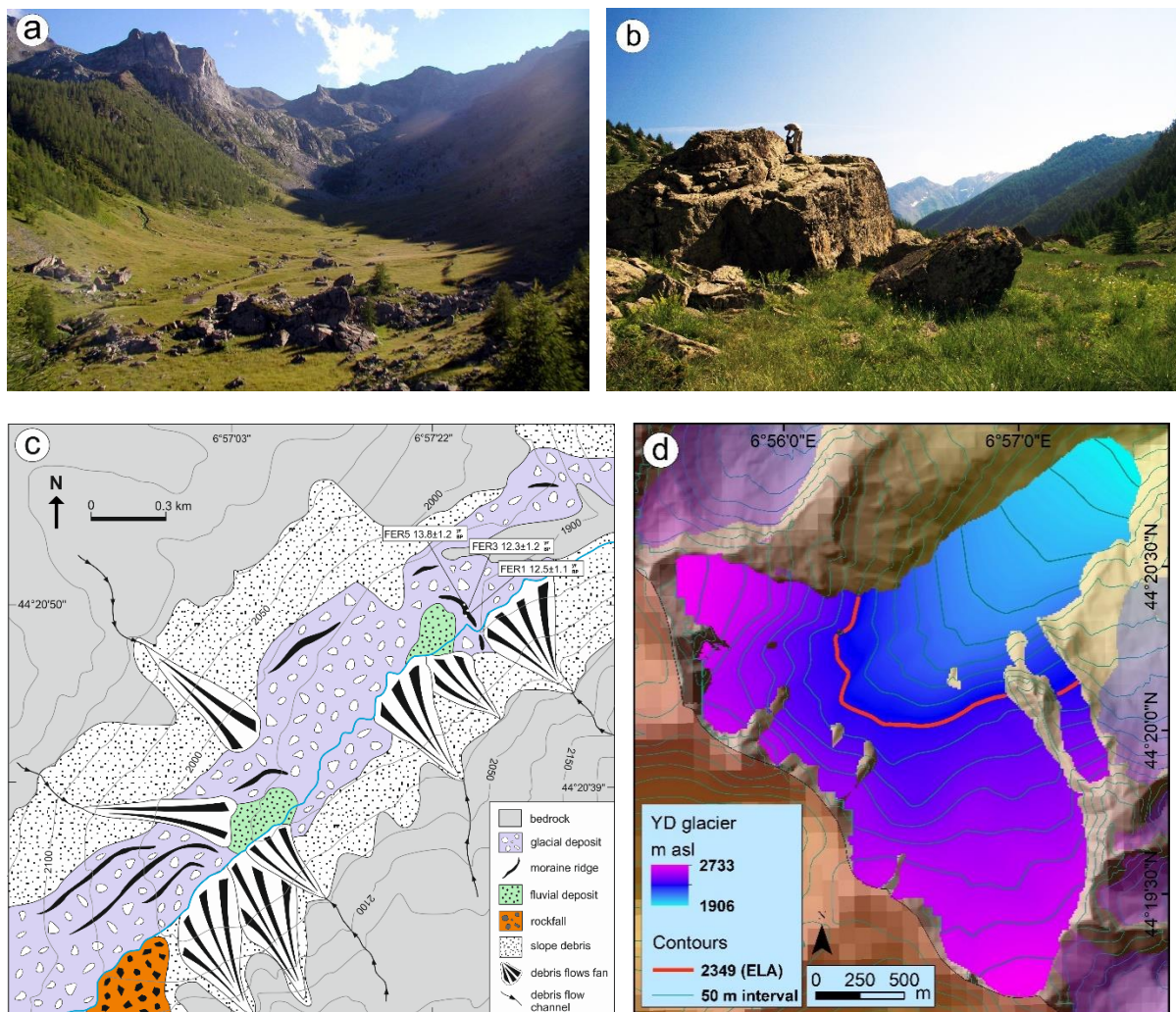
171

172 3.3 Palaeoclimatology

173 The climatological study is focused on the extraction of palaeoprecipitation at the YD ELA
174 (average of the two ELAs obtained from the reconstructed glaciers that deposited moraines dated
175 back to the YD in the Maritime Alps). This study is based on the empirical lawmicrocliamt connecting
176 annual precipitation (P_{ann} in mm) and mean air temperature during the melting period (the summer
177 in our case, T_{melt}) at the ELA, following the equation $P_{ann} = 5.87 T_{melt}^2 + 230 T_{melt} + 966$ (Ohmura and
178 Boettcher, 2018). The temperature of the hottest month (T_{Jul}) for the YD in the region is sourced from
179 chironomids (midges), a fossil palaeotemperature proxy commonly found in freshwater lake deposits.
180 The chironomid series closest to the Maritime Alps and covering the YD period is found 95 km to the
181 north, at Lago Piccolo di Avigliana (45.0549°N, 7.3919°E; 365 m asl) (Larocque and Finsinger, 2008). At
182 this site, the average YD T_{Jul} is 16.3°C. In order to adjust this value to the elevation of the YD average
183 ELA we apply the present-day global lapse rate (6.5°C / 1km). While T_{Jul} is a good proxy for the
184 maximum monthly temperature and is very close to T_{melt} , for a precise calculation of the latter, T_{Jun}
185 and T_{Aug} also need to be taken into account and the temperature of the three months averaged. This
186 is achieved here by fitting a sine curve to the value of T_{Jul} and to the minimum monthly temperature
187 (T_{Jan}) (Brugger, 2006; Hughes and Braithwaite, 2008). The latter is obtained from a pollen study
188 conducted in one of the many lakes of the Stura catchment, the Orgials Lake, at 2240 m asl (Figure 1)
189 (Ortu et al., 2008). The average YD T_{Jan} for this site is -16.9°C, which is adjusted to the elevation of the

190 calculated YD ELA by using the standard lapse rate of 6.5°C / 1km. An attempt was also made to
 191 calculate T_{melt} with a different approach, based on a combination of the same chironomid data
 192 mentioned above and sea surface temperatures measured in northern Sicily (Cacho et al., 2001) and
 193 adjusted for the latitude and altitude of the ELA. However, the result is very similar to that obtained
 194 when combining chironomids with pollen data and, for the sake of clarity, we prefer to focus on the
 195 latter, which is based on proxies collected within or relatively close to the region of study.

196 In order to put the reconstructed YD palaeoclimate into context, we compare our calculation
 197 with present day measurements from a site within the Maritime Alps characterised by an elevation
 198 relatively close to the YD average ELA, namely the Diga del Chiotas weather station, which is at 1980
 199 m asl (Figure 1). Total annual precipitation, as well as January, July and summer (June-August)
 200 temperatures are averaged from 2001 to 2018 measurements. The measured temperatures are
 201 adjusted to the elevation of the calculated YD ELA by applying the standard lapse rate of 6.5°C / 1km.
 202



203
204

205
206
207
208
209

Figure 2 An overview of the Ferrere moraine and of the Forneris glacier: (a) Val Forneris and Ferrere moraine in the foreground; (b) FER3 sampled boulder on the crest of the moraine (notice one of us over its top for scale); (c) geomorphological map of the Ferrere moraine and surroundings, with indication of the position of the three

210 dated boulder samples; (d) reconstructed YD Forneris glacier that deposited the Ferrere moraine and the
 211 calculated YD ELA (thick red line) obtained by using the AABR technique.

213 4. Results

214 4.1 The Ferrere moraine and its age

215 FER is mainly composed of diamicton, with small (cms to dms) blocks immersed in abundant
 216 fine sediments. However, the most distinct trait of FER is the presence of a few, very large, angular
 217 blocks, with dimensions of up to 8 meters (Figure 2a, b). The blocks stand out of the ground and are
 218 aligned for about 350 m following a classic arcuate shape, typical of many marginal moraines. The
 219 frontal moraine deposit has clearly acted as a barrier to the natural flow of the main river, which now
 220 cuts the moraine into two halves. The relatively flat area right upvalley from the moraine is therefore
 221 characterised by a mixture of diamicton and fluvial sediments. The portion of other, less well
 222 preserved, lateral and frontal moraines exists in the immediate (~500 m) surroundings of FER (Figure
 223 2c), thus suggesting that multiple, most likely related to the same climatic event, glacier fluctuations
 224 (retreats and re-advances to a similar position) have occurred.

225 The Ferrere moraine samples, FER1, FER3 and FER5, returned ages of $12,490 \pm$ (external
 226 uncertainty, i.e. the sum of accelerator mass spectrometry measurement and production rate
 227 uncertainties) 1120 yr, $12,260 \pm 1220$ yr and $13,840 \pm 1240$ yr, respectively (Table 1). All three ages
 228 overlap in the 12,605-13,476 yr interval, with a weighted mean (\pm weighted standard deviation) of
 229 $12,950 \pm 700$ yr (calculated with iceTEA, Jones et al., 2019), and are therefore compatible with the YD
 230 timeframe. The FER ages are also similar to those of the other Maritime Alps moraine (PDP) dated
 231 back to the YD, which returned an average age of 13,174 yr (Federici et al., 2017).

232

| | FER1 | FER3 | FER5 |
|-----------------------------------|-------------|-------------|-------------|
| longitude (degrees) | 6.957441 | 6.957648 | 6.957622 |
| latitude (degrees) | 44.347136 | 44.347302 | 44.347483 |
| strike of sampled surface | horizontal | 310N | 70N |
| dip of sampled surface | flat | 8 SW | 20 SE |
| elevation (m asl) | 1908 | 1916 | 1915 |
| shielding factor (including self) | 0.943 | 0.942 | 0.933 |
| height of boulder (m) | 1.5-2.5 | 3-6 | 2-5 |
| sample thickness (cm) | <3 | <3 | <3 |
| rock type | gneiss | gneiss | gneiss |
| ¹⁰ Be (atoms/g) | 215,914 | 213,360 | 238,158 |
| ¹⁰ Be yr | 12,489 | 12,257 | 13,843 |
| internal uncertainty (years) | 321 | 621 | 355 |
| external uncertainty (years) | 1117 | 1219 | 1238 |

233

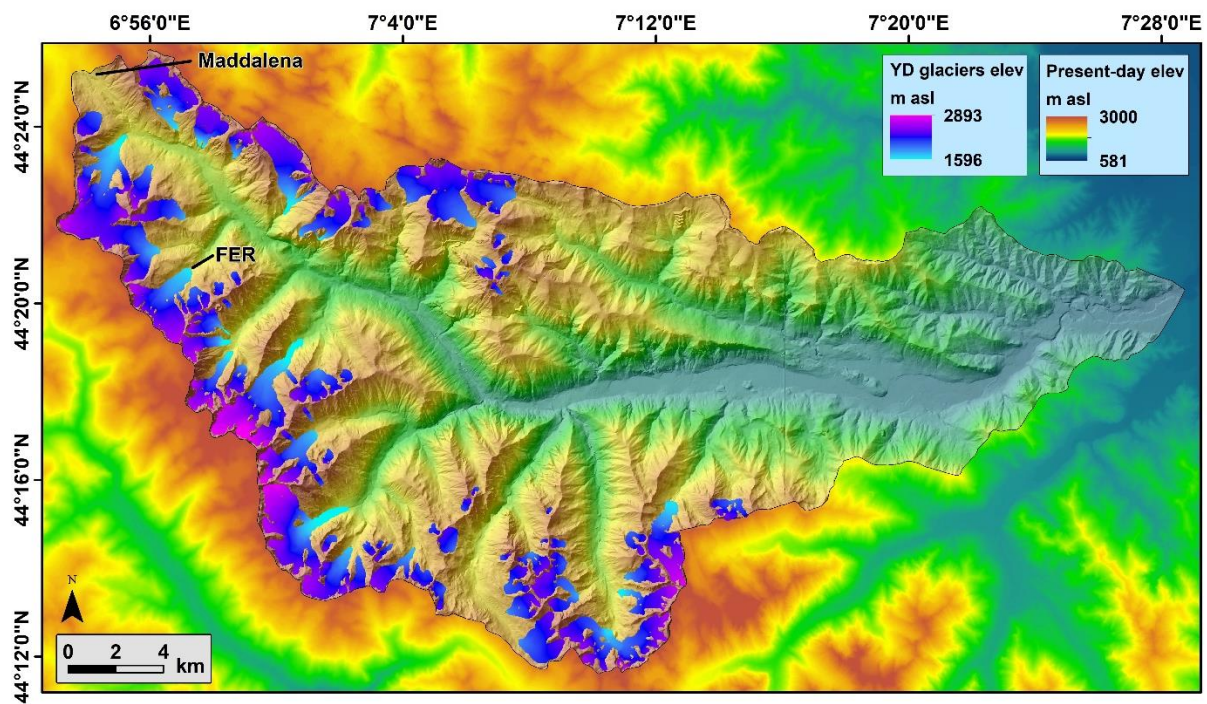
234 Table 1 Detail of the three boulder samples from the moraine near the village of Ferrere, in Val Forneris,
235 including their ¹⁰Be concentration and exposure age.

236

237

238 4.2 YD glaciers and ELA in the Maritime Alps

239 Identification of the Ferrere moraine, along with other glacial features, allowed for the
240 reconstruction of the glacier responsible for its deposition, called here the Forneris glacier after the
241 name of the valley. The reconstructed YD Forneris glacier (Figure 2d) has a length of 3.6 km from its
242 margin (at ~1906 m asl) to a point close to the valley divide (at ~2733 m asl), covering an elevation
243 range of 827 m. The glacier surface is 3.89 km² and its volume is 0.19 km³. The YD (AABR) ELA for the
244 reconstructed Forneris glacier is 2349 ± 5 m asl. The ELA of the other Maritime Alps glacier with a
245 moraine (PDP) dated to the YD, reconstructed with the same approach used here, is 2368 ± 5 m asl
246 (Federici et al., 2017). The two ELAs define a Maritime Alps YD ELA interval of 2344-2373 m asl, with
247 an average value of 2358 ± 15 m asl. The extent of 66 other potential YD glaciers was modelled across
248 the Stura catchment by iteratively changing their frontal position until their ELA fell within the 2344-
249 2373 m asl interval (Figure 3 and Table 2). The area of the 66 glaciers ranges from 0.07 km² (Lake
250 Sauma glacier) to 5.99 km² (Bernolfo glacier). Collectively, their area is 83.74 km² and the volume is
251 5.39 km³, equivalent to 4.94 Gt of water.



252

253 Figure 3 The 66 reconstructed YD glaciers in the Stura catchment of the Maritime Alps. “FER” indicates the
254 position of the Ferrere moraine, while “Maddalena” (or Larche) refers to the major ice-free pass across this
255 sector of the Alps at the YD.

256

257

258 *4.3 Palaeo- and present-day climate at the Maritime Alps YD ELA*

259 The YD average T_{Jul} at 2358 ± 15 m asl, the Maritime Alps YD ELA, calculated from the Lago
260 Piccolo di Avigliana chironomid study (Larocque and Finsinger, 2008), is 3.3 ± 1 °C. The YD average T_{Jan} ,
261 obtained from the Lago dell'Orgials pollen study (Ortu et al., 2008), is -17.7 ± 0.1 °C, thus defining a
262 seasonality ($T_{Jul} - T_{Jan}$) of 21.0 °C. With this, it is possible to estimate a T_{melt} of 2.4 ± 1 °C and a P_{ann} of
263 1549 ± 26 mm/yr, by applying a sine curve to model the monthly air temperature and the Ohmura and
264 Boettcher (2018) equation.

265 The present-day (2001-2018) precipitation at the nearby Diga del Chiotas weather station (1980 m asl,
266 i.e. 378 m lower than the YD ELA) is 1487 mm/yr and the January, July and summer (June-August)
267 temperatures are -1.7°C, 13.8°C and 12.8°C, respectively. These temperatures, when adjusted to the
268 elevation of the YD average ELA using the standard lapse rate, return values of -2.8°C, 11.4°C and
269 10.4°C respectively, with a seasonality of 14.2°C.

270

| Glacier name | Longitude (°E) | Latitude (°N) | Area (km ²) | Volume (km ³) | AABR ELA (m asl) | Reconstructed glacier front morphology |
|---------------------------|-------------------|------------------|----------------------------|------------------------------|---------------------|---|
| Orgials | 7.147 | 44.210 | 2.231 | 0.107 | 2346 | Moraine |
| Aver West | 7.137 | 44.223 | 0.928 | 0.037 | 2346 | - |
| San Giovanni | 7.133 | 44.233 | 0.755 | 0.029 | 2351 | - |
| Maladecia | 7.143 | 44.240 | 0.641 | 0.021 | 2357 | - |
| Argentera | 6.942 | 44.369 | 1.389 | 0.080 | 2359 | - |
| Bandia | 7.093 | 44.378 | 3.366 | 0.360 | 2352 | - |
| Becco Nero | 7.075 | 44.382 | 1.733 | 0.360 | 2373 | - |
| Bernolfo | 7.015 | 44.251 | 5.991 | 0.407 | 2373 | Glacial deposit |
| Bersezio | 6.982 | 44.396 | 0.632 | 0.014 | 2370 | - |
| Claval | 7.025 | 44.304 | 1.655 | 0.055 | 2354 | Moraine |
| Guercia | 7.050 | 44.233 | 0.606 | 0.025 | 2369 | Glacial deposit |
| Collalunga - San Bernolfo | 7.035 | 44.232 | 2.360 | 0.407 | 2348 | Moraine |
| Cologna | 7.055 | 44.375 | 0.563 | 0.018 | 2356 | - |
| Fauniera | 7.115 | 44.380 | 2.314 | 0.360 | 2358 | - |
| Ferrere | 6.927 | 44.355 | 2.897 | 0.150 | 2351 | moraine |
| Forneris | 6.945 | 44.334 | 3.893 | 0.195 | 2349 | moraine |
| Malinvern | 7.186 | 44.211 | 4.727 | 0.188 | 2364 | Glacial deposit |
| Paùr | 7.203 | 44.227 | 1.370 | 0.052 | 2367 | moraine |
| Aver East | 7.153 | 44.229 | 1.669 | 0.083 | 2360 | - |
| Perdù | 7.201 | 44.237 | 0.927 | 0.031 | 2357 | - |
| Martel | 7.155 | 44.240 | 0.473 | 0.083 | 2353 | Rock glacier |
| Giordano | 7.031 | 44.368 | 1.881 | 0.118 | 2346 | - |
| Ischiator | 7.013 | 44.277 | 2.677 | 0.112 | 2362 | Moraine |
| Lose | 6.931 | 44.378 | 0.951 | 0.034 | 2361 | - |
| Clamp | 7.195 | 44.249 | 0.466 | 0.015 | 2348 | Glacial deposit |
| Faniet | 6.973 | 44.341 | 0.199 | 0.005 | 2353 | - |
| Ventassuso | 6.903 | 44.402 | 0.820 | 0.030 | 2358 | - |
| Rocco Verde East | 6.977 | 44.335 | 0.088 | 0.001 | 2355 | Glacial deposit |
| Claval South | 7.021 | 44.294 | 0.104 | 0.002 | 2354 | Glacial deposit |
| Saletta | 7.033 | 44.278 | 0.175 | 0.004 | 2357 | Moraine |
| Maladecia west | 7.127 | 44.242 | 0.088 | 0.002 | 2348 | - |
| Cairillera East | 7.154 | 44.247 | 0.203 | 0.005 | 2354 | Moraine |
| Reduc | 7.244 | 44.262 | 0.832 | 0.027 | 2349 | - |
| Cairillera West | 7.147 | 44.248 | 0.046 | 0.001 | 2361 | - |
| Bravaria | 7.106 | 44.261 | 0.166 | 0.004 | 2372 | Rock glacier |
| Clarnier | 7.149 | 44.260 | 0.047 | 0.001 | 2353 | Rock glacier |
| Lausfer | 7.092 | 44.227 | 0.415 | 0.020 | 2364 | - |
| Passo Lausfer | 7.083 | 44.234 | 0.513 | 0.018 | 2371 | - |
| Mouton West | 7.089 | 44.252 | 0.131 | 0.004 | 2346 | Rock glacier |
| Mouton East | 7.097 | 44.248 | 0.676 | 0.049 | 2358 | Moraine |
| Steliere | 7.110 | 44.267 | 0.064 | 0.001 | 2352 | Moraine |
| Pignal | 7.063 | 44.242 | 0.196 | 0.004 | 2351 | Moraine |
| Lake Sauma | 7.061 | 44.245 | 0.071 | 0.001 | 2368 | Glacial deposit |
| Vallonet | 7.055 | 44.244 | 0.187 | 0.005 | 2360 | Moraine |
| Rocca Bernolfo | 7.034 | 44.246 | 0.251 | 0.006 | 2357 | Rock glacier |
| Loroussa South | 7.028 | 44.269 | 0.109 | 0.002 | 2370 | Glacial deposit |
| Cavias | 7.041 | 44.309 | 0.206 | 0.007 | 2349 | Rock glacier |
| Bassura North | 6.982 | 44.345 | 0.154 | 0.003 | 2360 | Rock glacier |
| Moura | 7.122 | 44.348 | 0.110 | 0.080 | 2365 | - |
| Nebius | 7.119 | 44.343 | 0.122 | 0.002 | 2348 | - |
| Oserot | 7.006 | 44.389 | 3.679 | 0.241 | 2373 | - |
| Stau North | 6.960 | 44.335 | 0.427 | 0.022 | 2352 | Moraine |
| Pilone | 6.965 | 44.337 | 0.289 | 0.022 | 2369 | Moraine |
| Peroni | 6.966 | 44.402 | 1.541 | 0.146 | 2372 | - |
| Piz | 6.995 | 44.297 | 5.657 | 0.381 | 2370 | - |
| Ponte Bernardo | 6.969 | 44.304 | 1.600 | 0.043 | 2371 | - |
| Puriac | 6.908 | 44.375 | 6.373 | 0.373 | 2347 | Glacial deposit |
| Roburent | 6.943 | 44.415 | 3.363 | 0.155 | 2362 | - |
| Nebius North | 7.114 | 44.351 | 0.450 | 0.080 | 2349 | - |
| Scoletta | 6.984 | 44.306 | 0.643 | 0.016 | 2355 | - |
| Serour | 7.120 | 44.361 | 0.174 | 0.005 | 2366 | - |
| Tesina | 7.067 | 44.235 | 1.216 | 0.057 | 2354 | Moraine |
| Valletta | 7.212 | 44.248 | 2.839 | 0.168 | 2349 | Moraine |
| Panieris | 6.964 | 44.319 | 1.111 | 0.037 | 2368 | - |
| Stau | 6.967 | 44.328 | 0.969 | 0.018 | 2353 | - |
| Vallonetto | 7.048 | 44.368 | 0.346 | 0.007 | 2373 | Moraine |
| TOTAL | - | - | 83.743 | 5.394 | - | - |

271

272 Table 2 Name, midpoint coordinates, area, volume and ELA of 66 reconstructed YD glaciers in the Stura
273 catchment. The presence of a moraine, a rock glacier, or generic glacial deposit at the reconstructed glacier front
274 is also noted.

275

276 5. Discussion

277 Well-preserved moraines associated with the Egesen stadial, the last of the Lateglacial stadials
278 in the European Alps, are common (Ivy Ochs et al., 2009). They are recognised as the first prominent,
279 blocky, usually multi-crested moraine set that can be found downvalley from the Little Ice Age moraine
280 (Ivy-Ochs, 2015). The FER moraine fits this description: it is the first moraine set that can be found
281 (about 2 km) downvalley from the Holocene moraines in the Val Forneris; its aspect, characterised by
282 very large boulders, resembles that of many other Alpine Egesen moraines (see Figure 4 in Hormes et

283 [al., 2008](#)); the presence of nearby moraines, most likely connected to the same climatic event, is also
284 a typical trait of the Egesen geomorphological signature across the Alps ([Ivy Ochs, 2015](#)). A handful of
285 Egesen stadial moraines has so far been dated with cosmogenic isotope exposure dating techniques,
286 all returning an age compatible with the YD ([Baroni et al., 2017](#); [Böhlert et al., 2011a](#); [Cossart et al.,](#)
287 [2012](#); [Federici et al., 2008](#); [Hormes et al., 2008](#); [Ivy-Ochs et al., 1996](#); [2006](#); [2009](#); [Kelly et al., 2004](#);
288 [Moran et al., 2016](#); [Schindelwig et al., 2012](#)). The FER moraine, dated here to the YD, is an important
289 addition to this sparse database. It provides further evidence that the Egesen stadial in the European
290 Alps actually represents the glaciological and morphological expression of the YD cooling event. It also
291 allows for the reconstruction of several potential YD/Egesen glaciers within its neighbourhood and its
292 ELA can be used to extract YD climatic conditions in this sector of the Alps.

293

294 *5.1 Climate*

295 A proper comparison of ELA values across the Alps for the YD is beyond the scope of this work
296 and would require a consistent reconstruction of all YD palaeoglaciers and the extraction of their ELA
297 with a same approach. However, different ELA calculation approaches would typically account for ELA
298 discrepancy of the order of some tens of meters, for alpine valley glaciers of the size considered here
299 (e.g. [Federici et al., 2017](#); [Scotti et al., 2017](#)). The average ELA (2358 m asl) of the two YD reconstructed
300 glaciers of the Maritime Alps is a few hundred meters lower than the ELA reported from other Alpine
301 sectors for this same glacier stadial ([Baroni et al., 2017](#); [Scotti et al., 2017](#)). This difference is an order
302 of magnitude greater than a potential methodologically-related discrepancy, indicating that the
303 climatic conditions of the Maritime Alps at the YD were peculiar within the context of the Alps. In an
304 alpine environment, the ELA of a valley glacier is largely controlled by the summer temperature, which
305 influences glacier ablation; and by solid, typically winter, precipitation, which affects ice accumulation.
306 The lower YD ELA of the Maritime Alps therefore reflects lower summer temperature and/or higher
307 solid precipitation, relative to the rest of the Alps.

308 The climatic reconstruction attempted here shows increased seasonality (6.8°C higher,
309 relative to present-day measurements) and a considerable drop in temperature at the YD (8.1°C lower
310 in July and 14.9°C lower in January, relative to present-day measurements), in line with other Alpine
311 YD palaeoclimate studies (e.g. [Lotter et al., 2000](#); [Heiri et al., 2014b](#)). However, it is the relatively high
312 YD precipitation, comparable to the present-day precipitation, that makes the YD climate of the
313 Maritime Alps peculiar within the context of the wider Alps. This is in apparent disagreement with the
314 paradigm of a widespread arid YD across most of Europe and the Alps (e.g. [Heiri et al., 2014a and b](#);
315 [Magny et al., 2001](#)), including its SW sector ([Ortu et al., 2008](#); [Brisset et al., 2015](#)); however, a previous
316 attempt to reconstruct palaeoprecipitation based on YD glacier ELA has highlighted considerable

317 variability in the central Alps, including regions where YD precipitation was similar to, and even higher
318 than, present-day precipitation (Kerschner, 1981; Kerschner et al., 2000; Kerschner & Ivy-Ochs, 2008).

319 The Maritime Alps YD climate reconstruction is based on at least three aspects that can be
320 challenged. Firstly, the YD relationship between temperature and precipitation at the ELA may have
321 been different from today's. Nonetheless, it is hard to physically justify such a scenario, as the law is
322 robustly based on current worldwide empirical observations, not specific to an individual site and
323 considering multi-decadal data (Ohmura and Boettcher, 2018). Secondly, the chironomid-derived YD
324 T_{Jul} might reflect local conditions only, thus questioning its validity for the calculation of temperatures
325 for a site that is 95 km away and at an elevation almost 2000 m higher. Thirdly, the pollen-derived YD
326 T_{Jan} , although relative to a site located within the Maritime Alps and at an elevation similar to the YD
327 ELA, might not be reliable since the approach suffers from lack of good analogues, problems with
328 pollen taxa and complexity of mountain ecosystems (e.g. Ortu et al., 2006). Despite these potential
329 limitations, it should be noted that a recent study, based on fossil trees from a location ~90 km west
330 of our site, also indicates non-arid conditions for this region at the onset of the YD (Pauly et al., 2018).
331 These conditions are interpreted as the effect of more frequent and/or intense precipitations
332 originating from North Atlantic air masses, combined with more intense winter storms resulting from
333 the interaction between cold high-latitude and warm Mediterranean air masses, along the margin of
334 the southward-displaced polar front (Pauly et al., 2018). Such an interpretation fits very well with the
335 uniqueness of the Maritime Alps YD glaciers within the context of the wider Alpine region, because of
336 their closer proximity to both the Mediterranean Sea and the Atlantic Ocean.

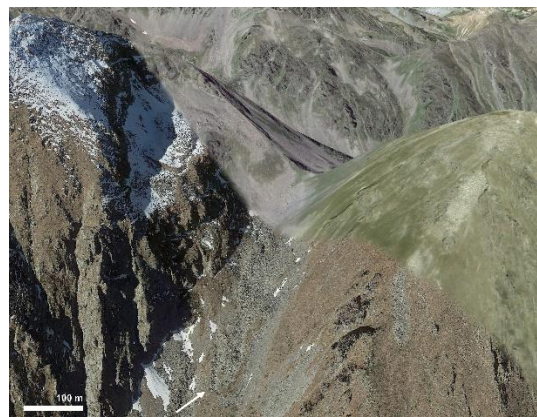
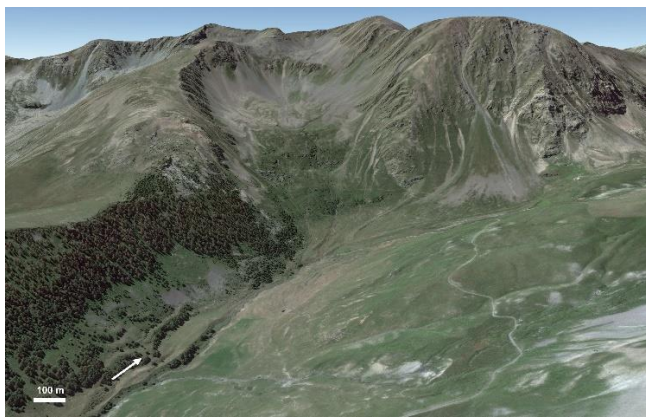
337

338 *5.2 Regional glaciers reconstruction*

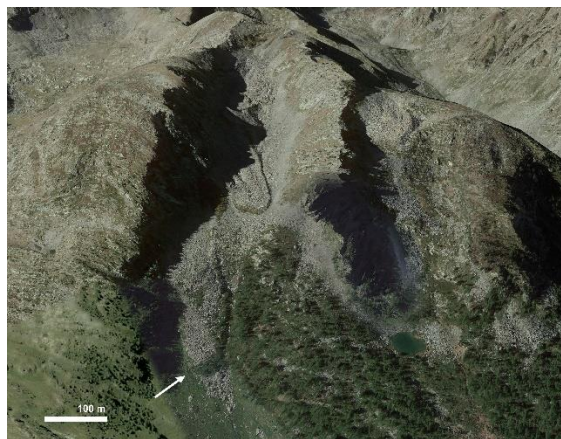
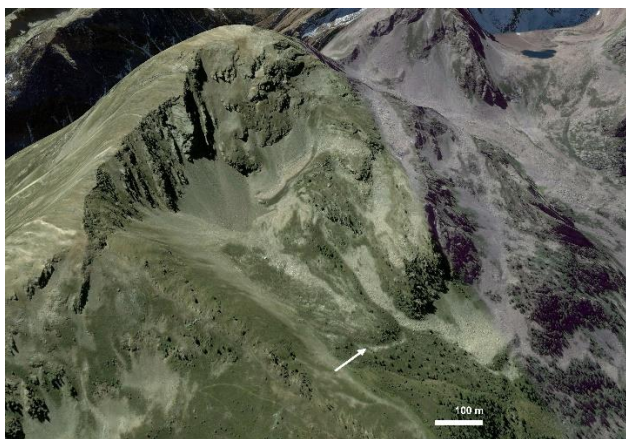
339 This paper represents the first attempt at using the GIS GlaRe tool (Pellitero et al., 2016) to model the
340 extent of all palaeoglaciers belonging to the same stadial in an extensive alpine region, using the ELA
341 of nearby palaeoglaciers associated with moraines also dated to that stadial. Although the trial-and-
342 error approach (by iteration of the glacier front position) is time-consuming, the reconstruction of 66
343 glaciers took some weeks against the months it would have probably taken using the classic manual
344 topographic approach (e.g. Porter et al., 1975; Carr et al., 2010), i.e. without the use of GlaRe. Most
345 importantly, GlaRe implements a physically-plausible plastic rheology glacier model for the glacier
346 reconstruction, thus giving further robustness to the results. The application of a regional ELA interval
347 defined by two dated moraines is questionable, since it is possible that ELA variability exceeded these
348 boundaries across the 66 glaciers. However, the defined interval allows us to provide a first order
349 model of the YD expansion and could be useful for further, more detailed studies.

350

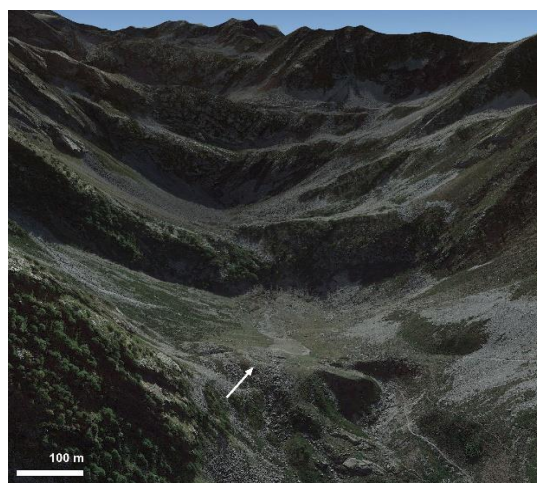
351



352



353



354 Figure 4. Examples of identified moraines on Google Earth™ located at the front (ice margin) of the
355 reconstructed YD glaciers in the Stura catchments. Top left: Ferrere glacier (the approximate coordinates of the
356 moraine are 44.35°N, 6.95°E); Top right: Laorussa South glacier (44.27°N, 7.03°E); Centre left: Saletta glacier
357 (44.28°N, 7.03°E); centre right: Pignal glacier (44.25°N, 7.07°E); Bottom left: Maladecia glacier (44.24°N, 7.14°E);
358 Bottom right: Valletta glacier (44.26°N, 7.21°E).

359

360

361

362

363

364

In order to test the modelled reconstruction presented here, the location of the 66-glacier front was checked in Google Earth™ and on an available geology map of the region that include some surface geology (Malaroda et al., 1970), with the aim to find evidence of a frontal moraine (Table 2). Twenty-nine percent of the settings have evidence of a moraine (Figure 4), while another 14% include glacial deposits where the morphology of a moraine could not be determined for sure, possibly an

365 issue related to the resolution of the available images. In some instances (another ~10% of the cases),
366 a rock glacier is found in the vicinity of the reconstructed glacier front, possibly incorporating a
367 potential YD moraine. This is in line with the evidence that the activity of many rock glaciers in the
368 Alps can be traced back to the end of the YD (Ivy-Ochs et al., 2009; Böhlert et al., 2011b; Moran et al.,
369 2016). The remaining 47% of reconstructed glaciers are characterised by the absence of a moraine or
370 a rock glacier at their front: in many instances, the resolution of the available imagery is either not
371 sufficiently high for the task, or the potential frontal moraine area is covered by thick vegetation. In
372 other, locations are clearly unsuitable for the deposition or preservation of a moraine, because the
373 valley bottom is particularly steep. If a moraine has not been identified, despite a favourable setting
374 and good imagery, the deposit might have been eroded by post-glacial events, buried by fluvial or
375 scree deposition. It is also possible that microclimatic condition (e.g. those potentially due to aspect)
376 might have resulted in a slightly longer or shorter glacier than the reconstructed one which is based
377 on a regional ELA and obtained using a tool, GlaRe, that does not take into consideration valley aspect.
378 In the future, it would be interesting to improve testing by undertaking extensive field work to verify
379 all the percentages reported above and by exposure-dating the moraines that will be identified.
380 However, for the time being, it is encouraging to see that several potential YD moraines are present
381 in the location identified by our modelled reconstruction (Table 2; Figure 4). This suggests that GlaRe
382 could be used as a predictive tool for further geomorphological investigations specific to a glacial
383 stadial for which at least one, ideally some, reliable (i.e. connected to a dated moraine) glacier
384 reconstructions and ELA calculations are available within a same region. For example, this could be
385 very helpful to plan fieldwork aimed at reaching other glacier front sites in nearby valleys, where
386 potential moraines of the same age could be found, sampled and dated.

387 YD glacier expansion in the Stura catchment sector of the Alps was limited to about 6% of the
388 total catchment area and confined to the highest altitudes, between 1596 and 2893 m asl. This is a
389 considerable reduction when compared to the Last Glacial Maximum expansion, when the Stura, like
390 other nearby major catchments, was occupied by a system of interconnected glaciers covering most
391 of the catchment and extending downvalley to the mountain front at 700 m asl, i.e. almost reaching
392 the Po Plain (Federici et al., 2008, 2012, 2017). Our modelled reconstruction indicates that most YD
393 glaciers extended hundreds of metres up to a few kilometres beyond the cirques. Some neighbouring
394 valley glaciers were connected, but not extensively enough to justify a description of the Egesen glacial
395 stadial in the Maritime Alps as an ice field. Almost all Stura valleys were glaciated at the YD, thus
396 considerably limiting plant/animal/human interaction, migration, communication and trading
397 between the southern and norther sectors of this Alpine region. The configuration of the YD Stura
398 glaciers indicates that only one pass across the main Alpine divide was then ice-free, the

399 Maddalena/Larche (44.42°N, 6.90°E, 1996 m asl). This was most-likely due to its elevation, which is at
400 least 300 m lower than all other main divide passes along the Stura valleys, associated with a lack of
401 nearby, high-elevation valleys and peaks that could have sustained a glacier able to reach the pass.
402 Ice-free Alpine passes are known to have played a crucial role in influencing pastoralism and
403 transhumance in the Alps during the early Holocene (e.g. [Hafner and Schwörer, 2018](#)) and it is likely
404 that they also played a role in influencing YD human activity, typically hunting and gathering. While
405 there is only limited information available on early human presence in the Alps, evidence of YD
406 settlements (campsites) generally linked to seasonal hunting has been recorded from various Alpine
407 archaeological sites ([Mussi and Persani, 2011](#); [Weber et al., 2011](#)), including the Maritime Alps
408 ([Tzortzis et al., 2008](#)). Within this sector of the mountain chain, it is likely that human (and animal)
409 interaction and migration across the Alpine main divide during the YD were funnelled in the
410 Maddalena/Larche pass. This represents an ideal site for future palaeoecological, palaeozoological
411 and archaeological investigations.

412

413

414 6. Conclusions

415

416 • A new Egesen stadial moraine in the Maritime Alps is dated here to $12,950 \pm 700$ yr (weighted
417 mean value of three measurements \pm weighted standard deviation) by means of cosmogenic
418 isotope analysis, thus adding further evidence to the link between the Egesen stadial of the
419 European Alps and the YD cooling event.

420 • The YD glacier that deposited the moraine is reconstructed and its ELA calculated to 2349 ± 5
421 m asl. This value is very similar to the ELA (2368 ± 5 m asl) of another palaeoglacier that
422 deposited a moraine (PDP) dated to the YD, 40 km to the SW. The similarity between the two
423 ELA suggests that the region experienced similar climatic conditions during the YD.

424 • The average between the two ELAs (2358 ± 15 m asl), combined with palaeotemperature data
425 provided by independent proxies, is used to establish the Maritime Alps YD annual
426 precipitation at the ELA, 1549 ± 26 mm/yr, based on the empirical law that links temperature
427 and precipitation at the ELA. Unlike most other Alpine sectors and European regions where
428 the YD seems to be characterised by aridity, the reconstructed YD precipitation for the
429 Maritime Alps is similar to present-day precipitation. This peculiarity is most likely related to
430 the Maritime Alps crossroads position, which allowed the region to intercept cold and humid
431 air masses from the Atlantic Ocean, pushed south by the displaced polar front, and warm and
432 humid air masses from the nearby Mediterranean Sea.

433 • The YD ELA interval defined by the two dated moraines allows to model the extent of all
434 potential YD glaciers (66) in the Stura catchment. The modelled location of the glaciers' front
435 matched well with the position of actual frontal moraines and glacial deposits observed in the
436 valleys, thus demonstrating that GLARE can be used as a predictive, modelling tool. The
437 modelled glaciers occupied all valley heads in the catchment with only one notable ice-free
438 pass across the main Alpine divide, that of the Maddalena/Larche pass. This is an ideal site for
439 future archaeological, palaeocological and palaeozoological studies with a focus on YD cross-
440 Alpine interactions in the Maritime Alps.

441

442

443 ACKNOWLEDGEMENTS

444 We would like to acknowledge: Prof. Rea and Dr Pellitero for fruitful discussions on various aspects of this
445 work, and in particular on the use of glacier reconstruction and ELA GIS tools and extraction of climatic
446 variables at a glacier ELA; Dr Ortu for kindly providing easy access to pollen data and for discussions on the
447 climate of the Younger Dryas across the Alps; Prof. Edwards for discussions on pollen analyses; and Prof.
448 Federici, for inspiring glaciological research in this beautiful region. The constructive and useful feedback
449 provided by Dr Monegato and an anonymous reviewer is greatly appreciated. L. Cignoni is thanked for
450 reviewing the English. MS acknowledges support from NERC (CIAF 9092.1010).

451

452 REFERENCES

453 [Auer, I., Böhm, R., Jurkovic, A., Lipa, W., Orlik, A., Potzmann, R., Schöner, W., Ungersböck, M., Matulla,](#)
454 [C., Briffa, K., Jones, P. D., Efthymiadis, D., Brunetti, M., Nanni, T., Maugeri, M., Mercalli, L., Mestre, O.,](#)
455 [Moisselin, J.-M., Begert, M., Müller-Westermeier, G., Kveton, V., Bochnicek, O., Stastny, P., Lapin, M.,](#)
456 [Szalai, S., Szentimrey, T., Cegnar, T., Dolinar, M., Gajic-Capka, M., Zaninovic, K., Majstorovic, Z.,](#)
457 [Nieplova, E., 2007. HISTALP — 'Historical instrumental climatological surface time series of the Greater](#)
458 [Alpine Region 1760–2003'. *Int. J. Climatol.* 27, 17–46.](#)

459 [Badino, F., Ravazzi, C., Vallè, F., Pini, R., Aceti, A., Brunetti, M., Champvillair, E., Maggi, V., Maspero,](#)
460 [F., Perego, R., Orombelli, G., 2018. 8800 years of high-altitude vegetation and climate history at the](#)
461 [Rutor Glacier forefield, Italian Alps. Evidence of middle Holocene timberline rise and glacier](#)
462 [contraction. *Quat. Sci. Rev.* 185, 41–68.](#)

463 [Baroni, C., Casale, S., Salvatore, M.C., Ivy-Ochs, S., Christl, M., Carturan, L., Seppi, R., Carton, A., 2017.](#)
464 [Double response of glaciers in the Upper Peio Valley \(Rhaetian Alps, Italy\) to the Younger Dryas](#)
465 [climatic deterioration. *Boreas* 46, 783–798.](#)

466 [Benn, D.I., Hulton, N.R.J., 2010. An Excel™ spreadsheet program for reconstructing the surface](#)
467 [profile of former mountain glaciers and ice caps. *Comput. Geosci.* 36, 605–610.](#)

468 [Benn, D.I., Lehmkuhl, F., 2000. Mass balance and equilibrium line altitudes of glaciers in high mountain](#)
469 [environments. *Quat. Int.* 65, 15–29.](#)

470 [Bigot-Cormier, F., Braucher, R., Bourlès, D., Guglielmi, Y., Dubar, M., Stéphan, J.F., 2005. Chronological](#)
471 [constraints on processes leading to large active landslides. *Earth Planet. Sci. Lett.* 235, 141–150.](#)

- 472 Bini, A., Buoncristiani, J.-F., Couterrand, S., Ellwanger, D., Felber, M., Florineth, D., Graf, H.R., Keller,
473 O., Kelly, M., Schlüchter, C., Schoeneich, P., 2009. Die Schweiz Während des Letzzeitlichen
474 Maximums (LGM) 1:500 000. Federal Office of Topography, swisstopo, Wabern, Switzerland.
- 475 Böhlert, R., Egli, M., Maisch, M., Brandová, D., Ivy-Ochs, S., Kubik, P.W., Haeberli, W., 2011a.
476 Application of a combination of dating techniques to reconstruct the Lateglacial and early Holocene
477 landscape history of the Albula region (eastern Switzerland). *Geomorphology* 127, 1-13.
- 478 Böhlert, R., Compeer, M., Egli, M., Brandova, D., Maisch, M., Kubik, P.W., Haeberli, W., 2011b. A
479 combination of relative-numerical dating methods indicates two high Alpine rock glacier activity
480 phases after the glacier advance of the Younger Dryas. *Open Geogr. J.* 4, 115-130.
- 481 Boston, C. M., Lukas, S., Carr, S. J., 2015. A Younger Dryas plateau icefield in the Monadhliath, Scotland,
482 and implications for regional palaeoclimate. *Quat. Sci. Rev.* 108, 139-162
- 483 Brisset, E., Guiter, F., Miramont, C., Revel, M., Anthony, E. J., Delhon, C., Arnaud, F., Malet, E., de
484 Beaulieu, J.L., 2015. Lateglacial/Holocene environmental changes in the Mediterranean Alps inferred
485 from lacustrine sediments. *Quat. Sci. Rev.*, 110, 49-71.
- 486 Broecker, W.S., Denton, G.H., Edwards, R.L., Cheng, H., Alley, R.B., Putnam A.E., 2010. Putting the
487 Younger Dryas cold event into context. *Quat. Sci. Rev.* 29, 1078–1081.
- 488 Brugger, K.A., 2006. Late Pleistocene climate inferred from the reconstruction of the Taylor River
489 glacier complex, southern Sawatch Range, Colorado. *Geomorphol.* 75, 318-329
- 490 Cacho, I., Grimalt, J.O., Canals, M., Sbaffi, L., Shackleton, N.J., Schönfeld, J., Zahn, R., 2001. Variability
491 of the Western Mediterranean sea surface temperature during the last 25,000 years and its
492 connection with the Northern Hemisphere climatic changes. *Paleoceanography* 16, 40-52.
- 493 Carr, S.J., Lukas, S., Mills, S.C., 2010. Glacier reconstruction and mass-balance modelling as a
494 geomorphic and palaeoclimatic tool. *Earth Surf. Processes Landf.* 35, 1103-1115.
- 495 Casazza, G., Grassi, F., Zecca, G., Minuto, L., 2016. Phylogeographic Insights into a peripheral refugium:
496 the importance of cumulative effect of glaciation on the genetic structure of two endemic plants. *PLoS*
497 *One* 11, e0166983.
- 498 Clark, P.U., Dyke, A.S., Shakun, J.D., Carlson, A.E., Clark, J., Wohlfarth, B., Mitrovica, J.X., Hostetler,
499 S.W., McCabe, A.M., 2009. The Last Glacial Maximum. *Science* 325, 710-714.
- 500 Catto, N., Liverman, D.G.E., Bobrowsky, P.T., Rutter, N., 1996. Laurentide, cordilleran, and montane
501 glaciation in the western Peace River - Grande Prairie region, Alberta and British Columbia, Canada.
502 *Quat. Int.* 32, 21-32.
- 503 Cossart, E., Fort, M., Boursières, D., Braucher, R., Perrier, R., Siame, L., 2012. Deglaciation pattern during
504 the Lateglacial/Holocene transition in the southern French Alps. Chronological data and geographical
505 reconstruction from the Clarée Valley (upper Durance catchment, southeastern France). *Palaeogeogr.,*
506 *Palaeoclimatol., Palaeoecol.* 315, 109-123.
- 507 Durand, Y., Laternser, M., Giraud, G., Etchevers, P., Lesaffre, B., Mérindol, L., 2009. Reanalysis of 44 yr
508 of climate in the French Alps (1958–2002): methodology, model validation, climatology, and trends
509 for air temperature and precipitation. *J. Appl. Meteorol. Climatol.* 48, 429–449.

- 510 Ehlers, J., Gibbard, P.L., 2004. Quaternary glaciations-extent and chronology: Part I: Europe. Elsevier,
511 Amsterdam.
- 512 Federici, P.R., Pappalardo, M., Ribolini, A., 2003. Geomorphological map of the Maritime Alps Natural
513 Park (Argentera Massif, Italy) and surroundings. Colour map, 1:25.000 scale, S.EL.CA., Firenze.
- 514 Federici, P.R., Granger, D.E., Pappalardo, M., Ribolini, A., Spagnolo, M., Cyr, A. J., 2008. Exposure age
515 dating and Equilibrium Line Altitude reconstruction of an Egesen moraine in the Maritime Alps, Italy.
516 *Boreas* 37, 245–253.
- 517 Federici, P.R., Granger, D.E., Ribolini, A., Spagnolo, M., Pappalardo, M., Cyr, A.J., 2012. Last Glacial
518 Maximum and the Gschnitz stadial in the Maritime Alps according to ¹⁰Be cosmogenic dating. *Boreas*
519 41, 277-291.
- 520 Federici, P.R., Ribolini, A., Spagnolo, M., 2017. Glacial history of the Maritime Alps from the Last Glacial
521 Maximum to the Little Ice Age. *Geol. Soc. London, Special Publication* 433, 137–159.
- 522 Florineth, D., Schlüchter, C., 1998. Reconstructing the Last Glacial Maximum (LGM) ice surface
523 geometry and flowlines in the Central Swiss Alps. *Eclogae Geol. Helv.* 91, 391–407.
- 524 Furbish, D.J., Andrews, J.T., 1984. The use of hypsometry to indicate long term stability and response
525 of valley glaciers to changes in mass transfer. *J. Glaciol.* 30, 199–211.
- 526 Garnier, S., Alibert, P., Audiot, P., Prieur, B., Rasplus, J.-Y., 2004. Isolation by distance and sharp
527 discontinuities in gene frequencies: Implications for the phylogeography of an alpine insect species,
528 *Carabus solieri*. *Mol. Ecol.* 13, 1883-1897.
- 529 Golledge, N.R., Hubbard, A., Sugden, D.E., 2008. High-resolution numerical simulation of Younger
530 Dryas glaciation in Scotland. *Quat. Sci. Rev.* 27, 888-904.
- 531 Hafner, A., Schwörer, C., 2018. Vertical mobility around the high-alpine Schnidejoch Pass. Indications
532 of Neolithic and Bronze Age pastoralism in the Swiss Alps from paleoecological and archaeological
533 sources. *Quat. Int.* 484, 3-18.
- 534 Heiri, O., Brooks, S.J., Renssen, H., Bedford, A., Hazekamp, M., Ilyashuk, B., Jeffers, E.S., Lang, B.,
535 Kirilova, E., Kuiper, S., Millet, L., Samartin, S., Toth, M., Verbruggen, F., Watson, J.E., Van Asch, N.,
536 Lammertsma, E., Amon, L., Birks, H.H., Birks, H.J.B., Mortensen, M.F., Hoek, W.Z., Magyari, E., Munõz
537 Sobrino, C., Seppä, H., Tinner, W., Tonkov, S., Veski, S., Lotter, A.F., 2014a. Validation of climate model-
538 inferred regional temperature change for lateglacial Europe. *Nat. Comm.* 5, 4914.
- 539 Heiri, O., Koinig, K.A., Spötl, C., Barrett, S., Brauer, A., Drescher-Schneider, R., Gaar, D., Ivy-Ochs, S.,
540 Kerschner, H., Luetscher, M., Moran, A., Nicolussi, K., Preusser, F., Schmidt, R., Schoeneich, P.,
541 Schwörer, C., Sprafke, T., Terhorst, B., Tinner, W., 2014b. Palaeoclimate records 60-8 ka in the Austrian
542 and Swiss Alps and their forelands. *Quat. Sci. Rev.* 106, 186-205.
- 543 Heuberger, H., 1968. Die Alpengletscher im Spät- und Postglazial. *Eiszeitalter und Gegenwart* 19, 270–
544 275.
- 545 Hormes, A., Ivy-Och, S., Kubik, P.W., Ferreli, L., Michetti, A.M., 2008. ¹⁰Be exposure ages of a rock
546 avalanche and a late glacial moraine in Alta Valtellina, Italian Alps. *Quat. Int.* 190, 136–145.
- 547 Hughes, P.D., Braithwaite, R., 2008. Application of a degree-day model to reconstruct Pleistocene
548 glacial climates. *Quat. Res.* 69, 110-116.

- 549 Hughes, P.D., Gibbard, P.L., Ehlers, J., 2013. Timing of glaciation during the last glacial cycle: evaluating
550 the concept of a global 'Last Glacial Maximum' (LGM). *Earth-Sci. Rev.* 125, 171-198.
- 551 Hughes, P.D., Woodward, J.C., Gibbard, P.L., 2007. Middle Pleistocene cold stage climates in the
552 Mediterranean: new evidence from the glacial record. *Earth Planet. Sci. Lett.* 253, 50–56.
- 553 Isola, I., Ribolini, A., Zanchetta, G., Bini, M., Regattieri, E., Drysdale, R.N., Hellstrom, J.C., Bajo, P.,
554 Montagna, P., Pons-Branchu, E., 2019. Speleothem U/Th age constraints for the Last Glacial conditions
555 in the Apuan Alps, northwestern Italy. *Palaeogeog. Palaeoclimatol. Palaeoecol.* 518, 62-71
- 556 Isotta, F.A., Frei, C., Weigluni, V., Perčec Tadić, M., Lassègues, P., Rudolf, B., Pavan, V., Cacciamani,
557 C., Antolini, G., Ratto, S. M., Munari, M., Micheletti, S., Bonati, V., Lussana, C., Ronchi, C., Panettieri,
558 E., Marigo, G., Vertačnik, G., 2014. The climate of daily precipitation in the Alps: development and
559 analysis of a high-resolution grid dataset from pan-Alpine rain-gauge data. *Int. J. Climatol.* 34, 1657-
560 1675.
- 561 Ivy-Ochs, S. 2015. Glacier variations in the European Alps at the end of the last glaciation. *Cuad. Invest.*
562 *Geogr.* 41, 295– 315.
- 563 Ivy-Ochs, S., Schlüchter, C., Kubik, P. W., Synal, H.-A., Beer, J., Kerschner, H., 1996. The exposure age
564 of an Egesen moraine at Julier Pass, Switzerland, measured with the cosmogenic radionuclides ¹⁰Be,
565 ²⁶Al and ³⁶Cl. *Eclogae Geol. Helv.* 89, 1049–1063.
- 566 Ivy-Ochs, S., Kerschner, H., Reuther, A., Maisch, M., Sailer, R., Schaefer, J., Kubik, P.W., Synal, H.A.,
567 Schlüchter, C., 2006. The timing of glacier advances in the northern European Alps based on surface
568 exposure dating with cosmogenic ¹⁰Be, ²⁶Al, ³⁶Cl, and ²¹Ne. In: Siame, L.L., Bourle`s, D.L., Brown, E.T.
569 (Eds.), *In Situ-Produced Cosmogenic Nuclides and Quantification of Geological Processes*. *Geol. Soc.*
570 *Am. Special Paper* 415, pp. 43–60.
- 571 Ivy-Ochs, S., Kerschner, H., Maisch, M., Christl, M., Kubik, P. W., Schlüchter, C., 2009. Latest Pleistocene
572 and Holocene glacier variations in the European Alps. *Quat. Sci. Rev.* 28,
573 2137–2149.
- 574 Kelly, M.A., Kubik, P.W., Von Blankenburg, F., Schlüchter, C. 2004. Surface exposure dating of the Great
575 Aletsch Glacier Egesen moraine system, western Swiss Alps, using the cosmogenic nuclide ¹⁰Be. *J.*
576 *Quat. Sci.* 19, 431–441.
- 577 Kerschner, H. 1981. Outlines of the climate during the Egesen Advance (Younger Dryas, 1000-10000
578 BP) in the central Alps of the western Tyrol, Austria. *Z. Gletscherkd. Glazialgeol.* 16, 229-240.
- 579 Kerschner, H., Kaser, G., Sailer, R., 2000. Alpine Younger Dryas glaciers as paleo-precipitation gauges.
580 *Ann. Glaciol.* 31, 80–84.
- 581 Kerschner, H., Ivy-Ochs, S., 2008. Palaeoclimate from glaciers: Examples from the Eastern Alps during
582 the Alpine Lateglacial and early Holocene. *Glob. Planet. Chang.* 60, 58-71.
- 583 Kohl, C.P., Nishiizumi, K., 1992. Chemical isolation of quartz for measurement of in-situ -produced
584 cosmogenic nuclides. *Geochim. Cosmochim. Acta* 56, 3583-3587.
- 585 Johnsen, S.J., Dahl-Jensen, D., Gundestrup, N., Steffensen, J.P., Clausen, H.B., Miller, H., Masson-
586 Delmotte, V., Sveinbjörnsdottir, A.E., White, J., 2001. Oxygen isotope and palaeotemperature records
587 from six Greenland ice-core stations: Camp Century, Dye-3, GRIP, GISP2, Renland and NorthGRIP. *J.*
588 *Quat. Sci.* 16, 299–307.

- 589 Jones, R.S., Small, D., Cahill, N., Bentley, M.J., Whitehouse, P.L., 2019. iceTEA: Tools for plotting and
590 analysing cosmogenic-nuclide surface-exposure data from former ice margins. *Quat. Geochronol.* 51,
591 72-86.
- 592 Larocque, I., Finsinger, W., 2008. Late-glacial chironomid-based temperature reconstructions for Lago
593 Piccolo di Avigliana in the southwestern Alps (Italy). *Palaeogeogr. Palaeoclimatol. Palaeoecol.* 257,
594 207–223.
- 595 Lotter, A.F., Birks, H.J.B., Eicher, U., Hofmann, W., Schwander, J., Wick, L., 2000. Younger Dryas and
596 Allerod summer temperatures at Gerzensee (Switzerland) inferred from fossil pollen and cladoceran
597 assemblages. *Palaeogeogr., Palaeoclimatol., Palaeoecol.* 159, 349-361.
- 598 Magny, M., Guiot, J., Schoellammer, P., 2001. Quantitative Reconstruction of Younger Dryas to Mid-
599 Holocene Paleoclimates at Le Locle, Swiss Jura, Using Pollen and Lake-Level Data. *Quat. Res.* 56, 170-
600 180.
- 601 Malaroda, R., Carraro, F., Dal Piaz, G.B., Franceschetti, B., Sturani, C., Zanella, E., 1970. Carta Geologica
602 del Massiccio dell'Argentera alla scala 1:50 000 e Note Illustrative. *Mem. Soc. Geol. Ital.* 9, 557–663.
- 603 Meyer, M.C., Hofmann, Ch.-Ch., Gemmell, A.M.D., Haslinger, E., Häusler, H., Wangda, D., 2009.
604 Holocene glacier fluctuations and migration of Neolithic yak pastoralists into the high valleys of
605 northwest Bhutan. *Quat. Sci. Rev.* 28, 1217-1237.
- 606 Moran, A.P., Ivy-Ochs, S., Schuh, M., Christl, M., Kerschner, H., 2016. Evidence of central Alpine glacier
607 advances during the Younger Dryas-early Holocene transition period. *Boreas* 45, 398–410.
- 608 Mussi, M., Peresani, M., 2011. Human settlement of Italy during the Younger Dryas. *Quat. Int.* 242.
609 360-370.
- 610 Musumeci, G., Ribolini, A., Spagnolo, M., 2003. The effects of late Alpine tectonics in the morphology
611 of the Argentera Massif (Western Alps, Italy–France). *Quat. Int.* 101, 191–201.
- 612 Nishiizumi, K., Imamura, M., Caffee, M.W., Southon, J.R., Finkel, R.C., McAninch, J., 2007. Absolute
613 calibration of ¹⁰Be AMS standards. *Nucl. Instrum. Methods Phys. Res. B* 258, 403–413.
- 614 Ohmura, A., Kasser, P., Funk, M., 1992. Climate at the equilibrium line of glaciers. *J. Glaciol.* 38, 397–
615 411.
- 616 Ohmura, A., Boettcher, M., 2018. Climate on the equilibrium line altitudes of glaciers: theoretical
617 background behind Ahlmann's P/T diagram. *J. Glaciol.* 64, 489-505.
- 618 Ortu, E., Brewer, S., Peyron, O., 2006. Pollen-inferred palaeoclimate reconstructions in mountain
619 areas: Problems and perspectives. *J. Quat. Sci.* 21, 615-627.
- 620 Ortu, E., Peyron, O., Bordon, A., de Beaulieu, J.L., Siniscalco, C., Caramiello, R., 2008. Lateglacial and
621 Holocene climate oscillations in the South-western Alps: An attempt at quantitative reconstruction.
622 *Quat. Int.* 190, 71-88.
- 623 Osmaston, H., 2005. Estimates of glacier equilibrium line altitudes by the area_altitude, the
624 area_altitude balance ratio and the area_altitude balance index methods and their validation. *Quat.*
625 *Int.* 138, 22–31.
- 626 Paterson, W.S.B., 1994. *The Physics of Glaciers*, 3rd Edition Pergamon/Elsevier, London.

- 627 Patzelt, G., 1972. Die spätglazialen Stadien und postglazialen Schwankungen von Ostalpengletschern.
628 *Berichte der Deutschen Botanischen Gesellschaft* 85, 47-57.
- 629 Pauly, M., Helle, G., Miramont, C., Büntgen, U., Treydte, K., Reinig, F., Guibal, F., Sivan, O., Heinrich, I.,
630 Riedel, F., Kromer, B., Balanzategui, D., Wacker, L., Sookdeo, A., Brauer, A., 2018. Subfossil trees
631 suggest enhanced Mediterranean hydroclimate variability at the onset of the Younger Dryas. *Sci. Rep.*
632 8, 13980.
- 633 Pellitero, R., Rea, B.R., Spagnolo, M., Bakke, J., Hughes, P., Ivy-Ochs, S., Lukas, S., Ribolini, A., 2015. A
634 GIS tool for automatic calculation of glacier equilibrium-line altitudes. *Comput. Geosci.* 82, 55-62.
- 635 Pellitero, R., Rea, B.R., Spagnolo, M., Bakke, J., Ivy-Ochs, S., Frew, C.R., Hughes, P., Ribolini, A., Lukas,
636 S., Renssen, H., 2016. GlaRe, a GIS tool to reconstruct the 3D surface of palaeoglaciers. *Comput.*
637 *Geosci.* 94, 77-85.
- 638 Porter, SC., 1975. Equilibrium line altitudes of late Quaternary glaciers in the Southern Alps, New
639 Zealand. *Quat. Res.* 5, 27– 47.
- 640 Ravazzi, C., Peresani, M., Pini, R., Vescovi, E., 2007. The Late Glacial in the Italian Alps and in the Po
641 Plain: Stratigraphy, vegetation history and human peopling [Il Tardoglaciale nelle Alpi e in Pianura
642 Padana. Evoluzione stratigrafica, storia della vegetazione e del popolamento antropico]. *Alpine*
643 *Mediterr. Q.* 20, 163-184.
- 644 Renssen, H., Mairesse, A., Goosse, H., Mathiot, P., Heiri, O., Roche, D.M., Nisancioglu, K.H., Valdes,
645 P.J., 2015. Multiple causes of the Younger Dryas cold period. *Nat. Geo.* 8, 946-949
- 646 Rea, B.R., 2009. Defining modern day area-altitude balance ratios (AABRs) and their use in glacier-
647 climate reconstructions. *Quat. Sci. Rev.* 28, 237–248.
- 648 Rea, B.R., Evans, D.J.A., 2007. Quantifying climate and glacier mass balance in north Norway during
649 the Younger Dryas. *Palaeogeogr. Palaeoclimatol. Palaeoecol.* 246, 307-330.
- 650 Ribolini, A., 2000. Relief distribution, morphology and Cenozoic differential uplift in the Argentera
651 Massif (French–Italian Alps). *Z. Geomorphol.* 44, 363–378.
- 652 Ribolini, A., Spagnolo, M., 2008. Drainage network geometry versus tectonics in the Argentera Massif
653 (French-Italian Alps). *Geomorphology* 93, 253–266.
- 654 Schindelwig, I., Akçar, N., Kubik, P.W., Schlüchter, C., 2012. Lateglacial and early Holocene dynamics
655 of adjacent valley glaciers in the Western Swiss Alps. *J. Quaternary Sci.* 27, 114-124.
- 656 Schönswetter, P., Stehlik, I., Holderegger, R., Tribsch, A., 2005. Molecular evidence for glacial refugia
657 of mountain plants in the European Alps. *Mol. Ecol.* 14, 3547-3555.
- 658 Schorr, G., Pearman, P.B., Guisan, A., Kadereit, J.W., 2013. Combining palaeodistribution modelling
659 and phylogeographical approaches for identifying glacial refugia in Alpine *Primula*. *J Biogeogr* 40,
660 1947–60.
- 661 Scotti, R., Brardinoni, F., Crosta, G.B., Cola, G., Mair, V., 2017. Time constraints for post-LGM landscape
662 response to deglaciation in Val Viola, Central Italian Alps. *Quat. Sci. Rev.*, 177, 10-33.
- 663 Seguinot, J., Ivy-Ochs, S., Jouvet, G., Huss, M., Funk, M., Preusser, F., 2018. Modelling last glacial cycle
664 ice dynamics in the Alps. *Cryosphere* 12, 3265-3285.

- 665 Serrano, E., Gómez-Lende, M., González-Amuchastegui, M.J., González-García, M., González-Trueba,
666 J.J., Pellitero, R., Rico, I., 2015. Glacial chronology, environmental changes and implications for human
667 occupation during the upper Pleistocene in the eastern Cantabrian Mountains. *Quat. Int.* 364, 22-34
- 668 Shakun, J. D., Carlson, A.E., 2010. A global perspective on Last Glacial Maximum to Holocene climate
669 change. *Quat. Sci. Rev.* 29, 1801-1816.
- 670 Shilling, D.H., Hollin, J.T., 1981. Numerical reconstructions of valley glaciers and small icecaps. In:
671 Denton, G. H., Hughes, T. J. (Eds.), *The Last Great Ice Sheets*. Wiley, New York, 207–220.
- 672 Spotl, C., Mangini, A., 2007. Speleothems and glaciers. *Earth Planet. Sci. Lett.* 254, 323-331.
- 673 Stehlik, I., 2003. Resistance or emigration? Response of alpine plants to the ice ages. *Taxon* 52, 499-
674 510.
- 675 Tzortzis, S., Mocci, F., Walsh, K., Talon, B., Court-Picon, M., Dumas, V., Py Saragaglia, V., Richer, S.,
676 2008. Les massifs de l'Argentiérois du Mésolithique au début de l'Antiquité: au croisement des
677 données archéologiques et paléoenvironnementales en haute montagne (Hautes-Alpes, parc national
678 des Ecrins). *Le peuplement de l'arc alpin*. Paris, Éd. du CTHS, 2008, p. 123-148.
- 679 van der Bilt, W.G.M., Rea, B.R., Spagnolo, M., Roerdink, D.L., Jørgensen, S.L., Bakke, J., 2018. Novel
680 sedimentological fingerprints link shifting depositional processes to Holocene climate transitions in
681 East Greenland. *Glob. Planet. Chang.* 164, 52-64.
- 682 Weber, M.-J., Grimm, S.B., Baales, M., 2011. Between warm and cold: Impact of the Younger Dryas on
683 human behavior in Central Europe. *Quat. Int.* 242, 277-301.
- 684
685
686
687